HHS Public Access

Author manuscript

Nanotoxicology. Author manuscript; available in PMC 2016 February 02.

Published in final edited form as:

Nanotoxicology. 2015 ; 9(8): 941–951. doi:10.3109/17435390.2014.984251.

Microvascular and mitochondrial dysfunction in the female F1 generation after gestational TiO_2 nanoparticle exposure

Phoebe A. Stapleton[1,2], **Cody E. Nichols**[1,3], **Jinghai Yi**[1,2], **Carroll R. McBride**[1,2], **Valerie C. Minarchick**[1,2], **Danielle L. Shepherd**[1,3], **John M. Hollander**[1,3], and **Timothy R. Nurkiewicz**[1,2]

[1]Center for Cardiovascular and Respiratory Sciences, West Virginia University School of Medicine, Morgantown, WV, USA

[2]Department of Physiology and Pharmacology, West Virginia University School of Medicine, Morgantown, WV, USA

[3]Division of Exercise Physiology, West Virginia University School of Medicine, Morgantown, WV, USA

Abstract

Due to the ongoing evolution of nanotechnology, there is a growing need to assess the toxicological outcomes in under-studied populations in order to properly consider the potential of engineered nanomaterials (ENM) and fully enhance their safety. Recently, we and others have explored the vascular consequences associated with gestational nanomaterial exposure, reporting microvascular dysfunction within the uterine circulation of pregnant dams and the tail artery of fetal pups. It has been proposed (*via* work derived by the Barker Hypothesis) that mitochondrial dysfunction and subsequent oxidative stress mechanisms as a possible link between a hostile gestational environment and adult disease. Therefore, in this study, we exposed pregnant Sprague-Dawley rats to nanosized titanium dioxide aerosols after implantation (gestational day 6). Pups were delivered, and the progeny grew into adulthood. Microvascular reactivity, mitochondrial respiration and hydrogen peroxide production of the coronary and uterine circulations of the female offspring were evaluated. While there were no significant differences within the maternal or litter characteristics, endothelium-dependent dilation and active mechanotransduction in both coronary and uterine arterioles were significantly impaired. In addition, there was a significant reduction in maximal mitochondrial respiration (state 3) in the left ventricle and uterus. These studies demonstrate microvascular dysfunction and coincide with mitochondrial inefficiencies in both the cardiac and uterine tissues, which may represent initial evidence that prenatal ENM exposure produces microvascular impairments that persist throughout multiple developmental stages.

Correspondence: Timothy R. Nurkiewicz, PhD, Center for Cardiovascular and Respiratory Sciences, West Virginia University,1 Medical Center Drive, Robert C. Byrd Health Sciences Center, Morgantown, WV 26506-9105, USA. Tel: (304) 293-7328. Fax: (304) 293-5513. tnurkiewicz@hsc.wvu.edu.

Declaration of interest

The authors report no conflicts of interest.

Supplementary material available online Supplementary Figures 1–4.

Keywords

Barker Hypothesis; engineered nanomaterials; nanotoxicology; pregnancy; prenatal

Introduction

Maternal health status and lifestyle during pregnancy have been hypothesized as the fetal basis of adult disease (Capra et al., 2013) and is commonly termed the ‘‘Barker Hypothesis’’ (Fall et al., 1995; Hales & Barker, 1992). A fundamental mechanism proposed by the Barker Hypothesis is fetal development within a hostile gestational environment may lead to metabolic or physiologic adaptations, which foster adult disease (Simmons, 2012). However, the mechanistic connections between the prenatal intrauterine milieu and susceptibility to adult disease are poorly understood (Rogers & Velten, 2011). Recently, models representing fetal programming through the Barker Hypothesis mechanistically link the presentation of adult disease, with mitochondrial abnormalities (mitochondrial dysfunction and development of reactive oxygen species (ROS)) that stem from fetal development in a hostile gestational environment (Andreux et al., 2013). Mitochondrial dysfunction and inefficiencies leading to ROS production and subsequent nitric oxide (NO) quenching has been hypothesized as a major disrupter of normal microvascular reactivity (Mann et al., 2012; Nurkiewicz et al., 2009; Stapleton et al., 2012b).

Given the ever advancing and constantly expanding field of nanotechnology, there is an increasing demand to assess the nanotoxicological outcomes in non-traditional populations in order to fully consider the potential and enhance the safety of engineered nanomaterials (ENM). Recently, the National Institute of Environmental Health and Safety announced an initiative to evaluate fetal toxicity, teratology and the genetic basis of adult disease (National Institute of Environmental Health Sciences, 2012). This has lead to a handful of initial studies to address this call (Hougaard et al., 2010, 2013; Jo et al., 2013; Stapleton et al., 2013; Yamashita et al., 2011). In our previous study, we reported maternal ENM exposure early in gestation impairs litter size and fetal growth while simultaneously interrupting conservation of mass (Stapleton et al., 2013). Therefore, we focus our current studies on exposure after a sufficient time has been allowed for embryonic implantation.

In this regard, gamete toxicology has been a primary avenue of study for many years with the evaluation of male (Braydich-Stolle et al., 2005) and female germline mutations (Boisen et al., 2012), sperm production (Kyjovska et al., 2013; Mathias et al., 2014; Yoshida et al., 2010) and female fertility (Hougaard et al., 2013). ENM have also been investigated as endocrine disrupters (Iavicoli et al., 2013) in the primary and subsequent F1 generations after ENM exposure. These endocrine disruptions may have profound effects on the functionality of the cardiovascular system and associated vascular reactivity of the reproductive system (Ruehlmann et al., 1998). While therapeutic applications of nanomaterials on the uterus are under investigation (Ali et al., 2013), there are currently no studies that have evaluated the toxicokinetics of ENM exposure on uterine microvascular function.

Nearly every pathologic condition has a microvascular origin and/or consequence; therefore, we and others have explored the vascular effects associated with nanomaterial exposure during pregnancy. These studies have reported reduced vascular smooth muscle (VSM) relaxation (dilation) and increased VSM contractility (Stapleton et al., 2013; Vidanapathirana et al., 2014) in the maternal uterine microcirculation and umbilical vein. Dysfunction at this critical stage of growth is capable of influencing uterine blood flow and this contribution to the development of a hostile gestational environment. It has also been established that maternal ENM exposure during gestation is capable of impairing fetal growth, development and maturation within this adverse intrauterine milieu (Stapleton et al., 2013; Vidanapathirana et al., 2014). Furthermore, we have reported that gestational ENM exposure leads to fetal vascular dysfunction within the tail artery (Stapleton et al., 2013). While maternal and fetal studies are ongoing, studies of the adult progeny outcomes stemming from *in utero* ENM exposure remain sparse, and it is unclear if this fetal microvascular dysfunction persists into adulthood.

Overall, the adult cardiovascular outcomes and mechanisms associated with development in an adverse uterine environment due to maternal ENM exposure have yet to be fully determined, much less applied to unique nanomaterial exposures and/or specific material characteristics. Our previous work with nanosized titanium dioxide (nano-TiO_2) inhalation over the past 10 years initially stem from use as a surrogate for ultrafine particulate matter and ultimately evolved into studies of direct occupational ENM exposures (LeBlanc et al., 2009; Nurkiewicz et al., 2004, 2011; Stapleton et al., 2014). In this study we chose to study the coronary microcirculation, as dysfunction in this cardiac tissue is most immediately associated with myocardial ischemia and infarction, whereas the uterine microcirculation as very few studies have directly assessed microvascular pathology specifically germane to the female reproductive system. Therefore, the purpose of this study was to establish the long-term health consequences suffered by the F1 generation after prenatal exposure to nano-TiO_2, with respect to the coronary and uterine microvasculature, and mitochondrial health. Our hypothesis was that *in utero* exposure to nano-TiO_2 leads to systemic microvascular dysfunction associated with mitochondrial inefficiencies, which contribute to an increase in oxidative stress production.

Methods

Animal model

Sprague-Dawley rats (250–275 g female; 300–325 g male) were purchased from Hilltop Laboratories (Scottsdale, PA). Rats were housed at West Virginia University with food and water provided *ad libitum* and acclimated for at least 72-hours before mating, as previously described (Stapleton et al., 2013). To increase the likelihood of viable progeny, pregnant rats were placed within the inhalation facility on or after implantation (gestational day 6) as indications of inhalation exposure prior results in near to total loss of implantation (data not shown). Weights of the pregnant dams were recorded weekly. Dams delivered in-house and progeny grew to adulthood. Mothers were sacrificed after weaning, and the uterus was removed to visualize implantation sites by staining the uterus with 10% ammonium sulfate (Parker, 2006). The number of implantation sites were compared with the number of fully

developed pups within each litter to assess pup loss. Weights of the progeny were recorded weekly after weaning to monitor growth. The microvascular and mitochondrial studies were completed with female progeny between 11 and 16 weeks of age; however, some female littermates grew to 20 weeks of age and were included in the weights listed in Table 1. All procedures were approved by the Institutional Animal Care and Use Committee of the West Virginia University. The experimental design is depicted in Supplemental Figure 1.

Engineered nanomaterial

Nano-TiO_2 P25 powder was obtained from Evonik (Aeroxide TiO_2, Parsippany, NJ). This powder has previously been shown to be a mixture composed primarily of anatase (80%) and rutile (20%) TiO_2, with a primary particle size of 21 nm and a surface area of 48.08 m^2/g (Nurkiewicz et al., 2008; Sager & Castranova, 2009; Sager et al., 2008). The nano-TiO_2 was prepared with care prior to aerosolization by drying, sieving and storing the powder (Knuckles et al., 2011; Nurkiewicz et al., 2008).

Inhalation exposure

The nanoparticle aerosol generator was developed, designed and tested specifically for rodent nanoparticle inhalation exposures (US patent application # US13/317,472) (Yi et al., 2013). It consists of a vibrating fluidized bed cylinder with a baffle, a vibrating Venturi disperser and a cyclone separator. Nano-TiO_2 aerosols generated from the bulk dry powder were diluted and delivered to the animal inhalation exposure chamber at 90 LPM. The test atmospheres were monitored in real time with the ELPI (Dekati, Tampere, Finland) and adjusted manually to assure a consistent and known exposure for each experimental animal group. During the inhalation exposure, the actual concentrations were measured using gravimetric methods, three to four measurements were taken for calculating inhaled dose. The particles were collected on 47 mm PTFE membrane filters. A XP2U microbalance (Mettler Toledo, Küsnacht, Switzerland) was used to weigh the fillers.

Once a steady-state aerosol concentration was achieved, exposure duration was adjusted to achieve a daily calculated deposition of 43.8 ± 1.2 μg. Pregnant animals were placed within the inhalation chamber and exposed for five hours per day for an average of 6.8 ± 0.5 days at a final mass concentration of 10.6 ± 0.3 mg/m^3 or to filtered air (0 mg/m^3, control). Tremendous care was taken to achieve the same final mass concentration for each consecutive day of exposure. Our ability to reliably and repeatably characterize the aerosols in real time using ELPI and SMPS (TSI Inc., St. Paul, MN) enables us to achieve this day-to-day consistency (Yi et al., 2013). All animals received their final inhalation exposure within at least 24-hours of litter delivery.

Calculated total deposition was calculated based on mouse methodology previously described and normalized based on rat weight and to pregnant rat minute ventilation (Leavens et al., 2006; Porter et al., 2012; Stapleton et al., 2012a) using the following equation: $D = F \times V \times C \times T$, where F is the deposition fraction (10%), V is the minute ventilation based on body weight, C equals the mass concentration (mg/m^3) and T equals the exposure duration (minutes) (Nurkiewicz et al., 2008). The aerosol characterization can be found in Supplemental Figure 2.

Tissue preparation

Female progeny were anesthetized with isoflurane (5% induction, 2% maintenance) and placed on a heating pad to maintain 37 °C rectal temperature. The carotid artery and trachea were carefully intubated for the acquisition of mean arterial pressure and heart rate, as previously described (LeBlanc et al., 2009, 2010; Minarchick et al., 2013; Stapleton et al., 2012a). These measurements were recorded by PowerLab830 (AD Instruments, Colorado Springs, CO). The uterus and heart were removed, respectively, flushed of excess blood and placed in individual dishes of dish of chilled (4 °C) physiological salt solution [PSS (in mmol/L): 129.8 NaCl, 5.4 KCl, 0.5 NaH_2PO_4, 0.83 $MgSO_4$, 19 $NaHCO_3$, 1.8 $CaCl_2$ and 5.5 glucose]. Rats were euthanized upon removal of the heart.

Microvessel isolation

Microvascular heterogeneity—Heterogeneity can be considered characterized by branching patterns, pressure profiles, volume flow, vasoactive influences and/or receptor distributions/sensitivities within a microvascular bed (Tuma et al., 2008). As no two beds are identical, microvascular networks are considered considerable heterogenetic. Therefore, due to this heterogeneity, we consider these microvascular beds and the arterioles within these networks to be considered independent observations; where meaningful differences can be missed if the responses of multiple vessels from a single animal (or multiple) are pooled.

Coronary—Within the epicardium, arterioles (5150 mm maximum diameter) 3–4 branch orders down from the left anterior descending (LAD) artery were isolated and transferred to a vessel chamber (Living Systems Instrumentation, Burlington, VT), cannulated with glass pipettes, secured using nylon suture (11-0 ophthalmic, Alcon, Surrey, UK), and superfused with warmed (37 °C) oxygenated (21% O_2 – 5% CO_2 – 74% N_2) PSS at a rate of 10 mL/min. These arterioles were extended to their *in situ* length and pressurized to 45 mm Hg with PSS and allowed to develop spontaneous tone (Chilian et al., 1986; Stapleton et al., 2012a).

Uterine—As previously stated (Stapleton et al., 2013), we consider premyometrial radial uterine arteries to be representative of the uterine microcirculation due to their anatomic position within the tissue, passive diameter and functional resistance. Therefore, the uterus was pinned to visualize the vasculature, and a distal segment of the radial artery was isolated, removed, transferred, cannulated and extended as described above. These radial arterioles were pressurized to 60 mm Hg due to their anatomical location and allowed to develop spontaneous tone as previously described (Barron et al., 2010; Stapleton et al., 2013).

All vessel diameters were measured using video calipers (Colorado Video, Boulder, CO). Following equilibration, arteriolar reactivity was randomly evaluated to ensure that responses were neither interactive nor time-dependent in response to: (1) luminal pressure changes to elicit a myogenic response (i.e. reductions and increases in pressure from 0 to 90 mm Hg (coronary) or 0 to 120 mm Hg (uterine) at 15 mm Hg increments); (2) endothelium-dependent dilator (acetylcholine (ACh) (10^{-9}–10^{-4} M)); (3) endothelium-independent dilator (spermine NONOate (SPR) (10^{-9}–10^{-4} M)); (4) vasoconstrictor (serotonin (5-HT)

(10^{-9}–10^{-4} M); and (5) blood flow-induced dilation (endothelial mechanotransduction to elicit a shear stress response by changes to luminal blood flow [reductions and increases in blood flow from 0 mL/min to 30 mL/min at 5 mL/min increments]). Following assessments of arteriolar reactivity, the superfusate was replaced with Ca^{2+}-free PSS until passive diameter could be established. Each vessel was exposed to 2–5 reactivity assessments in addition to spontaneous tone and passive diameter measurements; however, to prevent an ordering effect, vessels were exposed to a randomized order of agonists or mechanical conditions.

Reactivity assessment—Spontaneous tone was calculated by the equation: $[(D_M - D_I)/D_M] \times 100$, where D_M is the maximal diameter recorded at 45 mm Hg for the coronary and 60 mmHg for the uterine arterioles under Ca^{2+}-free PSS as described above, and D_I is the initial steady-state diameter achieved prior to experimental period. Vessels were included for study if spontaneous tone ≥ 20% was achieved.

The responses to ACh, 5-HT and SPR are presented as percent relaxation from spontaneous baseline diameter: $[(D_{SS} - D_{CON})/(D_M - D_{CON})] \times 100$, where D_{SS} remains the steady-state diameter achieved after each chemical bolus, and D_{CON} is the control diameter measured immediately prior to the dose-response experiment. All experimental periods were at least two minutes, and all steady-state diameters were collected for at least one minute. Therefore, we are able to normalize responses for potential differences in baseline diameters before each dose-response curve.

The myogenic index (MI) is a functional indicator of the slope of the active pressure–diameter relationship for an arteriole at a given pressure (Davis, 1993). This measurement was determined using the following equation: $MI = 100 \times [(r_f - r_i)/r_i]/(P_f - P_i)$, where r_f is the final radius, r_i is the initial radius, P_f is the final intraluminal pressure and P_i is initial intraluminal pressure. This type of evaluation allows for a quantitative assessment between groups. Overall, the greater the myogenic responsiveness within the raw data to a provided intraluminal pressure (not shown), the more negative the calculated MI value.

Shear stress was calculated according to the equation: $\tau = 4\eta Q/\pi r3$, where η represents viscosity (0.8 centipoise (cP)), Q represents volumetric flow rate (measured with a calibrated flow indicator, Living Systems Instrumentation) and r equals the vessel radius.

Mitochondrial isolation

Using the tissue harvested for the microvascular assessments, in combination with an additional subset of litters (three litters in the control and two in the exposed), the mitochondria were isolated from the left ventricle of the heart as previously described (Palmer et al., 1977) with modifications by our laboratory (Dabkowski et al., 2009). Briefly, these tissues were excised, minced and homogenized in cold Chappell–Perry buffer [containing (in mmol/l) 100 KCl, 40 Tris·HCl, 10 Tris base, 5 $MgCl_2$, 1 ATP and 1 EDTA; pH 7.4], supernatants were then extracted and centrifuged to isolate mitochondria and maximize mitochondrial yield (Dabkowski et al., 2009). Mitochondrial pellets were resuspended in KME buffer (100 mM KCl, 50 mM MOPS and 0.5 mM EDTA) for mitochondrial respiration and ROS production measurements on freshly isolated samples.

Uterine mitochondria were isolated following similar procedures, excluding protease treatment. Mitochondrial pellets were resuspended in KME buffer (100 mM KCl, 50 mM MOPS and 0.5 mM EDTA) for mitochondrial respiration and ROS production measurements. Protein content was determined by the Bradford method using bovine serum albumin as a standard (Bradford, 1976).

There are two populations of mitochondria within the left ventricle of the heart. The interfibrillar (IFM) are located between the myofibrils of the cardiomyocyte are more compact and have a higher respiration (Hollander et al., 2014), whereas the subsarcolemmal (SSM) population are located beneath the cardiomyocyte membrane. Using this methodology where the entirety of the left ventricle is homogenized, the internal IFM population is purely cardiomyocyte derived; however, as the SSM population is more superficial, it may also include a small number of mitochondrial derived from other cells within the left ventricle (e.g. neural, VSM and endothelial cells). This tissue of the uterus is not known to have these differing populations. Due to this, we will refer to the mitochondria as either cardiac- or uterine-derived.

Mitochondrial respiration

State 3 and 4 respiration rates were assessed in isolated mitochondrial subpopulations as previously described (Chance & Williams, 1955, 1956; Hofhaus et al., 1996) with slight modifications (Dabkowski et al., 2009). After the mitochondrial isolation, equal amounts of protein were resuspended in respiration buffer containing 80 mmol/l KCl, 50 mmol/l MOPS, 1 mmol/l EGTA, 5 mmol/l KH_2PO_4 and 1 mg/ml BSA, which were then loaded into a Qubit OX1LP-1 mL dissolved oxygen chamber (Qubit System, Kingston, ON, Canada) attached to a Qubit biological oxygen monitor and Vernier LabPro system (Vernier Software and Technology, Beaverton, OR). The substrates glutamate (5 mM) + malate (5 mM) were used to initiate maximal respiration, and measurements of state 3 (1 mM ADP) and state 4 (ADP-limited) respiration were made as previously described (Chance & Williams, 1955).

Hydrogen peroxide production

Hydrogen peroxide production was assayed using fresh samples acquired from either the left ventricle or uterus and a fluorogenic indicator, Amplex red (10-acetyl-3,7-dihydroxyphenoxazine), in the presence of horseradish peroxidase as described (Votyakova & Reynolds, 2001; Zhou et al., 1997).

Statistical analysis

Data are expressed as mean ± standard error, where "*n*" represents the number of rats studied and "*n*" represents the number of arterioles evaluated as previously described (Boegehold, 1998; Nurkiewicz et al., 2008; Stapleton et al., 2013). In this study, the experimental unit was the arteriole, with one to three microvessels studied per rat for the uterine and/or coronary studies, or in combination. Therefore, these arterioles are considered to be independent observations due to the considerable heterogeneity within the microvascular bed.

Student's *t*-test was used to detect significance between sham and prenatally exposed animal and vessel characteristics in addition to the mitochondrial and hydrogen peroxide data ($p<0.05$), except with respect to the categorical data (e.g. sex of the pups) where a Pearson's Chi-square test was used. Concentration-diameter (ACh, 5-HT and SPR) and mechanotransduction (flow-diameter and MI) curves were assessed by a two-way analysis of variance. In all cases, Student–Newman–Keuls *post hoc* test was used when appropriate, and $p<0.05$ was taken to reflect statistical significance. Equations of first-order regression lines were developed to assess line slope relationships (SigmaPlot 11.0, Systat Software, San Jose, CA) and a Student's *t*-test was used to determine significance ($p<0.05$).

Results

To allow for implantation, pregnant dams were placed into the inhalation chamber after gestational day 6, where they were exposed to nano-TiO_2 aerosols or filtered air. After normal delivery, female rats were used for the purpose of this study. There were no significant differences in the sexes within the sham (46% female) and/or control (48% female) litters. It is important to reiterate when referencing the findings in this manuscript, we are referring to the female adult F1 generation of rats after *in utero* ENM exposure.

Supplemental Figure 2 is a graphical representation of nano-TiO_2 characterization. The primary particle diameter is 21 nm; however, as these particles tend to agglomerate during aerosolization, the average aerodynamic diameter of 149.1 nm± 3.7, is consistent with other experiments within our research program (Knuckles et al., 2011; Stapleton et al., 2013; Yi et al., 2013). The calculated total deposition and calculated deposition after clearance are presented in Supplemental Figure 2C.

There were no significant differences between the litters with respect to maternal weight, implantation sites, litter size, sex of pups or female progeny weight gain, or progeny age at the time of study (Table 1). The progeny were between 11 and 16 weeks of age at the time of study (Table 1). This age range is considered sexually mature and has not demonstrated any vascular differences associated with growth during young adulthood (Linderman & Boegehold, 1999).

There were no significant differences in spontaneous active diameter, passive diameter or vascular tone with respect to coronary arterioles between the sham and prenatal exposure groups (Table 2). However, there were significant differences within the uterine radial artery active diameter and spontaneous vessel tone between exposure groups, but not the passive maximal diameters. These differences indicate prenatal ENM exposure may induce a compensatory stimulus that leads to a larger active arteriolar diameter and decreased uterine vascular tone compared with control.

Coronary (Figure 1A) and uterine (Figure 1B) endothelium-dependent arteriolar dilation in the adult F1 generation is abolished after prenatal ENM exposure, a condition indicative of severe endothelial dysfunction. This dysfunction may be attributed to altered NO signaling, due to decreased NO bioavailability commonly associated with oxidative NO scavenging. Alternatively, this dysfunction, most notably the robust vasoconstriction observed within the

coronary arterioles at [Ach]>10^{-6} may be the result of endothelial production of contractile factors.

Epicardial arteriolar endothelium-independent dilation was blunted after pre-natal nanomaterial exposure at physiologically relevant concentrations (Figure 1C). The response within the gestational exposure group paralleled control levels at high doses. However, the biological relevance of this response remains unclear. Uterine arteriolar responsiveness to increased NO bioavailability remains unchanged, indicative of a functional NO signaling cascade and appropriate smooth muscle relaxation (Figure 1D). While using a point-by-point analysis may yield significance at the 10^{-4} M dosage, the physiological relevance of this type of analysis is unclear.

5-HT is a potent vasoconstrictor in the heart and uterus and was used to evaluate VCM contractile responses. There are no significant differences between the vasoconstrictive responses to 5-HT in either tissue (Supplemental Figure 3). This suggests that agonists stimulated VSM contractility is not altered in either tissue of the prenatally exposed adult F1 generation.

There were no significant differences with respect to myogenic responsiveness within the coronary microvessels (Figure 2A). However, there were significant differences within the uterine groups at physiologically relevant pressures (30, 60, 90 and 120 mm Hg) indicating a reduced myogenic responsiveness within the radial arterioles of the prenatally exposed animals (Figure 2B).

Both coronary (Supplemental Figure 4A) and uterine (Supplemental Figure 4B) arterioles derived from prenatally exposed animals, demonstrate a dysfunctional vasoconstriction to increases in intraluminal flow (5–30 μL/min). Overall, the development of shear stress is a function of vessel diameter. Therefore shear stress calculations for coronary (Supplemental Figure 4C) and uterine (Supplemental Figure 4D) microvessels were plotted against increases in intraluminal flow and illustrating an increased shear stress generation within both of the prenatally exposed tissues. Finally, when relaxation is plotted as a function of shear stress, it is clear that the *in utero* exposure has a profound effect within the coronary (Figure 2C) and uterine (Figure 2D) microvasculature, leading to the development of abnormal shear stress generation (due to a lack of dilation). These differences are primarily due to a flow-induced constriction compared to the flow-induced dilation in control tissues.

Mitochondria isolated from the left ventricle of the heart indicate a significant decline in maximal (State 3) respiration of both the SSM and IFM mitochondrial subpopulations of the progeny exposed to ENM *in utero* (Figure 3A). In addition, this difference was evident in resting (State 4) respiration of the IFM.

To our knowledge, this is the first report to isolate and measure state 3/4 respiration of uterine mitochondria. These studies demonstrate a significant reduction in maximal (state 3) respiration in uterine derived mitochondria (Figure 3B). While not of concern during normal resting conditions, this metabolic inadequacy may be insufficient to support normal fetal development upon implantation. With respect to Amplex Red analysis, there were no

significant differences in the hydrogen peroxide production within any of the gross tissues (Figure 3C).

Discussion

To our knowledge, this is the first study to illustrate the direct applicability of the Barker Hypothesis to ENM exposure in terms of the long-term microvascular consequences associated with prenatal ENM exposure and offspring development. This dysfunction has been demonstrated in the heart and uterine arterioles of the F1 generation of rats exposed to nano-TiO_2 during gestation. Finally, we have provided mechanistic evidence that this dysfunction may be due to mitochondrial inefficiencies after such exposures.

The representative coronary arterioles isolated within this study are a downstream branch of the LAD artery, responsible for perfusion of the left ventricle. Ischemia or the inability of the vasculature to meet the demands of this highly metabolic tissue may lead to devastating consequences associated with left ventricular function, cardiac output, systemic blood flow and maintenance of blood pressure. Endothelial cell dysfunction has been identified as an initial symptom of cardiovascular disease (Schwartz, 1980; Stapleton et al., 2008). These outcomes may not be symptomatic at rest; however, when metabolic demand is increased (as with exercise or moderate activity), the system may not be able to meet said demand, leading to a condition of coronary ischemia. If the system is additionally stressed with the development of a range of cofactors (e.g. diabetes, hypercholesterolemia, obesity and pregnancy), the inability of the coronary vasculature to meet the demands of the heart may be fatal. While we and others have described coronary vascular dysfunction (LeBlanc et al., 2009; Stapleton et al., 2012a; Thompson et al., 2014) and cardiovascular responses (Roberts et al., 2013; Thompson et al., 2014) after primary or direct exposure, this is the first study to demonstrate coronary endothelial dysfunction after *prenatal* ENM exposure. This predisposition toward cardiovascular dysfunction could represent a risk factor to be further studied in future translational research.

It should be fully appreciated that alterations in endothelium-dependent dilation do not implicitly produce changes in arterial pressure, due to the fact that endothelium-dependent dilation does not singularly regulate basal tone, but is only a contributing factor. Neural, endocrine, metabolic and physical factors also play significant roles in *in vivo* net basal activity.

Within the uterine circulation, decreased basal tone, in combination with agonist (ACh) and mechanical (flow) endothelial cell dysfunction demonstrates evidence of a possible alteration in peripheral resistance *in vivo*. Considering these results, an inability to meet the metabolic demands of an implantation and/or developing fetus may jeopardize the health and support of F2 or future generations. Few groups have explored the vascular adaptations of the uterus associated with normal function (Osol & Moore, 2014) let alone after prenatal ENM exposure; however, the implications of disturbed uterine vascular reactivity in combination with coronary arteriolar dysfunction on future conception, implantation and successful gestation are all unknown. Uterine vascular remodeling during pregnancy, specifically of the uterine artery, is initiated in part, from downstream factors (Osol &

Moore, 2014); however, if these signals do not elicit the appropriate microvascular response, fetal metabolic demand may not be met. In this case, the development of a hostile gestational environment or intrauterine growth restriction impairing the maturity of the F2 generation is plausible. It is cautioned that reproductive and developmental studies are limited and therefore, at this time *in vivo* studies of well-characterized ENM are needed and warranted (Ema et al., 2010).

This is also the first study to report mitochondrial alterations associated with prenatal ENM exposure, as well as the first to report uterine mitochondrial data. The inefficiencies associated with gestational exposure were illustrated in the SSM and IFM populations of the left ventricle, along with the uterine tissue. State 3 and 4 respiratory measures are theoretical descriptors of mitochondrial function and describe maximal (state 3) and passive (state 4) mitochondrial state. Mitochondrial state 3 respiration is measured as ADP-stimulated oxygen consumption in the presence of excess substrates to identify the potential maximum respiratory rate of ATP production. In contrast, mitochondrial state 4 respiration is measured as ADP-limited mitochondrial respiration in which all other substrates are present but availability of ADP is limited; *in vivo*, mitochondrial respiration lies somewhere between these two states. A decrease in either respiratory capacity suggests mitochondrial inefficiencies leading to reduced ATP production. Considering the high-oxidative metabolism of the heart and the potential within the non-pregnant uterus, these inefficiencies may have a profound impact on bioenergetics and performance. While this finding did not alter the comparison between the control and exposed group, it is interesting to note that there was a significant difference within all the control mitochondrial groups (uterine, SSM and IFM) with respect to age (data not shown). However, alterations in developmental mitochondrial bioenergetics are outside the scope of this study and should be fully considered in future work.

With respect to the null results associated with oxidative stress analysis, this finding is based on tissue analysis and may not be fully representative of the ROS content *in vivo* within the vasculature of the tissues. Therefore, microvascular wall ROS measurements are needed to verify this possibility. In addition, these results do not eliminate ROS as a potential mechanism; at this point, they indicate that the hydrogen peroxide may not be the primary reactive species of interest. Future analyses may include direct measurements of superoxide, alternative byproducts (peroxynitrite) and/or enzymatic activities (myeloperoxidase/catalase).

With respect to the maternal exposure, we have previously reported that the human pulmonary exposure equivalent would be similar to a woman working eight hours per day at the National Institute for Occupational Safety and Health current recommended exposure limit for nano-TiO_2 (0.3 mg/m3) for approximately two weeks (Stapleton et al., 2013). In terms of the doses, our calculated daily pulmonary depositions were no more than ~100 micrograms nano-TiO_2/rat for the entirety of gestation (Stapleton et al., 2013). However, even if we assume zero pulmonary clearance over our multiple day of exposure, the highest net calculated pulmonary deposition would be ~400 micrograms nano-TiO_2, a value well below typical overload thresholds in the high milligram range (International Life Sciences Institute Risk Science Institute, 2000; Warheit et al., 2009). If this maximum maternal

deposition is considered to estimate biodistribution at the end of exposure/gestation (~300 mg nano-TiO_2, Supplemental Figure 2) and clearance is ignored, it has been estimated that an approximate dose in the range of 30–300 ng nano-TiO_2 would translocate to the maternal liver (Hougaard et al., 2010). Again, if one considers this translocated mass to then evenly distribute between the dam and the litter (presuming no translocation resistance from the placental barrier), it is unlikely at this time to detect any nano-TiO_2 in the F1 rats. This "worst" possible case speculation does not definitively establish that nano-TiO_2 does not translocate to the F1 generation, and indeed nominal amounts of nano-TiO_2 may be all that is necessary to alter fetal development in critical organs such as the brain, heart and/or liver that lead to long-lasting biological effects (neurological, cardiovascular and/or inflammatory). As such, future studies must focus directly on all periods of gestational development, with novel approaches and increased resolution.

The Barker Hypothesis is reemerging as a prominent theory to describe findings and outcomes associated with fetal programming during gestation. There is growing evidence of alterations to fetal "omics" (proteomics (Langley et al., 2013), epigenomics (Paneni et al., 2013), metabolomics (Fanos et al., 2013) and functional genomics (Ganesh et al., 2013)) playing an active role in the adult development of disease. In analyses using a "toxicogenomic approach", female offspring have been shown to be more sensitive to maternal exposure with respect to hepatic gene expression (Jackson et al., 2012). Due to recent technological developments, epigenetic evaluation of the progeny is warranted. Interestingly, as these mechanistic "omics" theories are not independent, future directions may also consider interrogations of the mitochondrial genome (Wallace, 2009).

Our findings in this study echo other maternal conditions or exposures, which are associated with the development of cardiovascular disease later in life including, but not limited to the following: preeclampsia (Giguere et al., 2012; Makikallio et al., 2012; Vedernikov et al., 1999), fetal growth restriction (Barker, 2006; Makikallio et al., 2012; Rogers & Velten, 2011), malnutrition (Gonzalez-Bulnes et al., 2013; Wu et al., 2004), chemical (nonylphenol) exposure (Chang et al., 2012) and air pollution (Backes et al., 2013; Ebisu & Bell, 2012; van den Hooven et al., 2012). As in this study, others have also linked the development of adult disease to an increase in oxidative stress generation from dysfunctional mitochondria (Simmons, 2012). However, while these correlative studies highlight dysfunctional physiology leading to the development of cardiovascular disease, they fail to examine the severity, onset or the mechanisms of dysfunction associated with the disease of the F1 generation.

The use of female models has been commonly avoided in biomedical research to reduce variability associated with reproductive hormones, creating an unmistakable disparity in the understanding of female implications associated with nanotoxicology. As the domestic and biomedical uses of these materials continue to evolve, so must our assessments. A past study from our group (Prisby et al., 2008) provides evidence of a protective mechanism in young females rats against cardiovascular consequences associated with direct diesel exhaust (phenanthraquinone) toxicant exposure. Therefore, future studies should consider a comparison of male/female outcomes in addition to the female estrous status within the

experimental design, while it was not in this study, leading to increased variation within each group, the overall significant differences between groups remain.

With respect to the litter characteristics, it is important to note that these exposures were limited to ensure successful gestation in effort to produce progeny for study. Preliminary exposures, prior to GD 6 and greater than seven days of exposure during gestation had led to severe impacts on litter health and fetal weights on gestational day 20 (Stapleton et al., 2013). Overall, we theorized these high exposures (both in dosage and time during gestation) would reduce the likelihood of implantation and thus restricting our acquisition of viable pups for this study. As maternal exposures can and do occur during any period of gestation, additional studies evaluating toxicokinetics during the entire pregnancy are recommended.

The novelty of the experimental design and the consideration of the F1 generation after ENM exposure lead to the possibility of numerous future studies. These include, but are not limited to, five major areas. First, generational models of exposure sensitization, wherein generations of prenatally exposed animals are returned to inhalation exposures in adulthood or through biomedical application (e.g. injection). Second, particle translocation during pregnancy/gestation leading to embryonic and/or placental targeting, shunted growth due to placental damage (Yamashita et al., 2011), developmental interference due to direct organ specific particle–tissue interaction and residual direct particle–tissue interactions into adulthood must be evaluated. Translocation may account for an increased hostile gestational environment due to physical (ENM deposition) and/or local oxidative and inflammatory signaling. While these local outcomes may seem minor with respect to maternal outcomes, they may have devastating consequences for a single developing fetus. Therefore, at this time, we cannot distinguish if these effects are a result of direct fetal targeting or development of a hostile gestational environment. Third, exploration of the inflammatory hypothesis as an influence of microvascular reactivity (Stapleton et al., 2012b) at each step of development (maternal gestation, fetal and adult) would lend invaluable data regarding the development of systemic inflammation after nanomaterial exposure and the propensity to carry a heightened inflammatory state through generations. In addition, alterations in behavior should be analyzed. Given the plausibility of ENM translocation to the developing fetus during gestational exposure (Jo et al., 2013) and the “immaturity” of the blood brain barrier during fetal development, it is conceivable that ENM could deposit within the brain during gestation. Considering the brain’s dependence on constant blood flow oxidative metabolism, subtle mitochondrial impairments may lead to significant behavioral alterations. At this time, only one study has reported the behavioral alterations are associated with prenatal exposure (Hougaard et al., 2010). Finally, the mitochondrial bioenergetics of these exposures must be thoroughly analyzed at each life stage (maternal, fetal and adult) to identify acute and chronic mitochondrial inefficiencies. These alterations may play a role in the development of a hostile gestational environment, in addition to contributing to the development of cardiovascular disease described in adulthood.

Conclusions

Our findings are consistent with previous reports describing fetal microvascular dysfunction after *in utero* ENM exposure (Stapleton et al., 2013), indicating that the Barker hypothesis is applicable after gestational EMN exposure. The mitochondrial dysfunction that results in the offspring of maternally exposed dams may have widespread cardiovascular impacts, most notably at the microvascular level studied herein. The persistence of this fetal microvascular dysfunction into adulthood may create the foundation for disease susceptibility, acceleration of pathologies and/or toxicant sensitization.

Supplementary Material

Refer to Web version on PubMed Central for supplementary material.

Acknowledgements

We thank Mr. Kevin Engels from the West Virginia University (WVU), Department of Physiology and Pharmacology, for his technical assistance in this study, specifically with our breeding program. We also thank Ms. Sara Lewis from the WVU Division of Exercise Physiology for her technical assistance with respect to the tissue preparation and mitochondrial isolations.

This study was supported by NIH-F32-ES023435 (PAS), R01-ES015022 (TRN), DP2DK083095 (JMH), T32-HL090610 (DLS), AHA-13PRE16850066 (CEN), NSF-1003907 (TRN, VCM) and DGE-1144676 (V. C. M., C. E. N. and T. R. N.).

References

Ali H, Kilic G, Vincent K, Motamedi M, Rytting E. Nanomedicine for uterine leiomyoma therapy. Ther Deliv. 2013; 4:161–75. [PubMed: 23343157]

Andreux PA, Houtkooper RH, Auwerx J. Pharmacological approaches to restore mitochondrial function. Nat Rev Drug Discov. 2013; 12:465–83. [PubMed: 23666487]

Backes CH, Nelin T, Gorr MW, Wold LE. Early life exposure to air pollution: how bad is it? Toxicol Lett. 2013; 216:47–53. [PubMed: 23164674]

Barker DJ. Adult consequences of fetal growth restriction. Clin Obstet Gynecol. 2006; 49:270–83. [PubMed: 16721106]

Barron C, Mandala M, Osol G. Effects of pregnancy, hypertension and nitric oxide inhibition on rat uterine artery myogenic reactivity. J Vasc Res. 2010; 47:463–71. [PubMed: 20431295]

Boegehold MA. Heterogeneity of endothelial function within the circulation. Curr Opin Nephrol Hypertens. 1998; 7:71–8. [PubMed: 9442366]

Boisen AM, Shipley T, Jackson P, Hougaard KS, Wallin H, Yauk CL, Vogel U. NanoTIO(2) (UV-Titan) does not induce ESTR mutations in the germline of prenatally exposed female mice. Part Fibre Toxicol. 2012; 9:19. [PubMed: 22656316]

Bradford MM. A rapid and sensitive method for the quantitation of microgram quantities of protein utilizing the principle of protein-dye binding. Anal Biochem. 1976; 72:248–54. [PubMed: 942051]

Braydich-Stolle L, Hussain S, Schlager JJ, Hofmann MC. In vitro cytotoxicity of nanoparticles in mammalian germline stem cells. Toxicol Sci. 2005; 88:412–19. [PubMed: 16014736]

Capra L, Tezza G, Mazzei F, Boner AL. The origins of health and disease: the influence of maternal diseases and lifestyle during gestation. Ital J Pediatr. 2013; 39:7. [PubMed: 23343462]

Chance B, Williams GR. Respiratory enzymes in oxidative phosphorylation. I. Kinetics of oxygen utilization. J Biol Chem. 1955; 217:383–93. [PubMed: 13271402]

Chance B, Williams GR. The respiratory chain and oxidative phosphorylation. Adv Enzymol Relat Subj Biochem. 1956; 17:65–134. [PubMed: 13313307]

Chang LL, Wun WS, Wang PS. In utero and neonate exposure to nonylphenol develops hyperadrenalism and metabolic syndrome later in life. I. First generation rats (F(1)). Toxicology. 2012; 301:40–9. [PubMed: 22765982]

Chilian WM, Eastham CL, Marcus ML. Microvascular distribution of coronary vascular resistance in beating left ventricle. Am J Physiol. 1986; 251:H779–88. [PubMed: 3766755]

Dabkowski ER, Williamson CL, Bukowski VC, Chapman RS, Leonard SS, Peer CJ, et al. Diabetic cardiomyopathy-associated dysfunction in spatially distinct mitochondrial subpopulations. Am J Physiol Heart Circ Physiol. 2009; 296:H359–69. [PubMed: 19060128]

Davis MJ. Myogenic response gradient in an arteriolar network. Am J Physiol. 1993; 264:H2168–79. [PubMed: 8322948]

Ebisu K, Bell ML. Airborne PM2.5 chemical components and low birth weight in the northeastern and mid-Atlantic regions of the United States. Environ Health Perspect. 2012; 120:1746–52. [PubMed: 23008268]

Ema M, Kobayashi N, Naya M, Hanai S, Nakanishi J. Reproductive and developmental toxicity studies of manufactured nanomaterials. Reprod Toxicol. 2010; 30:343–52. [PubMed: 20600821]

Fall CH, Osmond C, Barker DJ, Clark PM, Hales CN, Stirling Y, Meade TW. Fetal and infant growth and cardiovascular risk factors in women. BMJ. 1995; 310:428–32. [PubMed: 7873947]

Fanos V, Atzori L, Makarenko K, Melis GB, Ferrazzi E. Metabolomics application in maternal-fetal medicine. Biomed Res Int. 2013; 2013:720514. [PubMed: 23841090]

Ganesh SK, Arnett DK, Assimes TL, Basson CT, Chakravarti A, Ellinor PT, et al. Genetics and genomics for the prevention and treatment of cardiovascular disease: update: a scientific statement from the American Heart Association. Circulation. 2013; 128:2813–51. [PubMed: 24297835]

Giguere Y, Charland M, Theriault S, Bujold E, Laroche M, Rousseau F, et al. Linking preeclampsia and cardiovascular disease later in life. Clin Chem Lab Med. 2012; 50:985–93. [PubMed: 22107134]

Gonzalez-Bulnes A, Ovilo C, Lopez-Bote CJ, Astiz S, Ayuso M, Perez-Solana ML, et al. Fetal and early-postnatal developmental patterns of obese-genotype piglets exposed to prenatal programming by maternal over- and undernutrition. Endocr Metab Immune Disord Drug Targets. 2013; 13:240–9. [PubMed: 23808810]

Hales CN, Barker DJ. Type 2 (non-insulin-dependent) diabetes mellitus: the thrifty phenotype hypothesis. Diabetologia. 1992; 35:595–601. [PubMed: 1644236]

Hofhaus G, Shakeley RM, Attardi G. Use of polarography to detect respiration defects in cell cultures. Methods Enzymol. 1996; 264:476–83. [PubMed: 8965720]

Hollander JM, Thapa D, Shepherd DL. Physiological and structural differences in spatially-distinct subpopulations of cardiac mitochondria: influence of pathologies. Am J Physiol Heart Circ Physiol. 2014; 307:H1–14. [PubMed: 24778166]

Hougaard KS, Jackson P, Jensen KA, Sloth JJ, Loschner K, Larsen EH, et al. Effects of prenatal exposure to surface-coated nanosized titanium dioxide (UV-Titan). A study in mice. Part Fibre Toxicol. 2010; 7:16. [PubMed: 20546558]

Hougaard KS, Jackson P, Kyjovska ZO, Birkedal RK, De Temmerman PJ, Brunelli A, et al. Effects of lung exposure to carbon nanotubes on female fertility and pregnancy. A study in mice. Reprod Toxicol. 2013; 41:86–97. [PubMed: 23714338]

Iavicoli I, Fontana L, Leso V, Bergamaschi A. The effects of nanomaterials as endocrine disruptors. Int J Mol Sci. 2013; 14:16732–801. [PubMed: 23949635]

International Life Sciences Institute (ILSI) Risk Science Institute. The relevance of the lung response to particle overload for human risk assessment: a workshop consensus report. Inhal Toxicol. 2000; 12:1–17.

Jackson P, Hougaard KS, Vogel U, Wu D, Casavant L, Williams A, et al. Exposure of pregnant mice to carbon black by intratracheal instillation: toxicogenomic effects in dams and offspring. Mutat Res. 2012; 745:73–83. [PubMed: 22001195]

Jo E, Seo G, Kwon JT, Lee M, Lee B, Eom I, et al. Exposure to zinc oxide nanoparticles affects reproductive development and biodistribution in offspring rats. J Toxicol Sci. 2013; 38:525–30. [PubMed: 23824008]

Knuckles TL, Yi J, Frazer DG, Leonard HD, Chen BT, Castranova V, Nurkiewicz TR. Nanoparticle inhalation alters systemic arteriolar vasoreactivity through sympathetic and cyclooxygenase-mediated pathways. Nanotoxicology. 2011; 6:724–35. [PubMed: 21830860]

Kyjovska ZO, Boisen AM, Jackson P, Wallin H, Vogel U, Hougaard KS. Daily sperm production: application in studies of prenatal exposure to nanoparticles in mice. Reprod Toxicol. 2013; 36:88–97. [PubMed: 23295323]

Langley SR, Dwyer J, Drozdov I, Yin X, Mayr M. Proteomics: from single molecules to biological pathways. Cardiovasc Res. 2013; 97:612–22. [PubMed: 23180722]

Leavens TL, Parkinson CU, James RA, House D, Elswick B, Dorman DC. Respiration in sprague-dawley rats during pregnancy. Inhal Toxicol. 2006; 18:305–12. [PubMed: 22397324]

LeBlanc AJ, Cumpston JL, Chen BT, Frazer D, Castranova V, Nurkiewicz TR. Nanoparticle inhalation impairs endothelium-dependent vasodilation in subepicardial arterioles. J Toxicol Environ Health A. 2009; 72:1576–84. [PubMed: 20077232]

LeBlanc AJ, Moseley AM, Chen BT, Frazer D, Castranova V, Nurkiewicz TR. Nanoparticle inhalation impairs coronary microvascular reactivity via a local reactive oxygen species-dependent mechanism. Cardiovasc Toxicol. 2010; 10:27–36. [PubMed: 20033351]

Linderman JR, Boegehold MA. Growth-related changes in the influence of nitric oxide on arteriolar tone. Am J Physiol. 1999; 277:H1570–8. [PubMed: 10516197]

Makikallio K, Kaukola T, Tuimala J, Kingsmore F, Hallman M, Ojaniemi M. Umbilical artery chemokine CCL16 is associated with preterm preeclampsia and fetal growth restriction. Cytokine. 2012; 60:377–84. [PubMed: 22857868]

Mann EE, Thompson LC, Shannahan JH, Wingard CJ. Changes in cardiopulmonary function induced by nanoparticles. Wiley Interdiscip Rev Nanomed Nanobiotechnol. 2012; 4:691–702. [PubMed: 22915448]

Mathias FT, Romano RM, Kizys MM, Kasamatsu T, Giannocco G, Chiamolera MI, et al. Daily exposure to silver nanoparticles during prepubertal development decreases adult sperm and reproductive parameters. Nanotoxicology. 2014 [Epub ahead of print].

Minarchick VC, Stapleton PA, Porter DW, Wolfarth MG, Ciftyurek E, Barger M, et al. Pulmonary cerium dioxide nanoparticle exposure differentially impairs coronary and mesenteric arteriolar reactivity. Cardiovasc Toxicol. 2013; 13:323–37. [PubMed: 23645470]

National Institute of Environmental Health Sciences. Linking early environmental exposures to adult diseases. NIEHS; 2012. Available at: http://www.niehs.nih.gov/health/assets/docs_f_o/linking_early_environmental_exposures_to_adult_diseases.pdf. Accessed on 15 July 2014

Nurkiewicz TR, Porter DW, Barger M, Castranova V, Boegehold MA. Particulate matter exposure impairs systemic microvascular endothelium-dependent dilation. Environ Health Perspect. 2004; 112:1299–306. [PubMed: 15345343]

Nurkiewicz TR, Porter DW, Hubbs AF, Cumpston JL, Chen BT, Frazer DG, Castranova V. Nanoparticle inhalation augments particle-dependent systemic microvascular dysfunction. Part Fibre Toxicol. 2008; 5:1. [PubMed: 18269765]

Nurkiewicz TR, Porter DW, Hubbs AF, Stone S, Chen BT, Frazer DG, et al. Pulmonary nanoparticle exposure disrupts systemic microvascular nitric oxide signaling. Toxicol Sci. 2009; 110:191–203. [PubMed: 19270016]

Nurkiewicz TR, Porter DW, Hubbs AF, Stone S, Moseley AM, Cumpston JL, et al. HEI Health Review Committee. Pulmonary particulate matter and systemic microvascular dysfunction. Res Rep Health Eff Inst. 2011:3–48. [PubMed: 22329339]

Osol G, Moore LG. Maternal uterine vascular remodeling during pregnancy. Microcirculation. 2014; 21:38–47. [PubMed: 23941526]

Palmer JW, Tandler B, Hoppel CL. Biochemical properties of subsarcolemmal and interfibrillar mitochondria isolated from rat cardiac muscle. J Biol Chem. 1977; 252:8731–9. [PubMed: 925018]

Paneni F, Costantino S, Volpe M, Luscher TF, Cosentino F. Epigenetic signatures and vascular risk in type 2 diabetes: a clinical perspective. Atherosclerosis. 2013; 230:191–7. [PubMed: 24075743]

Parker, RM. Testing for reproductive toxicity. In: Ronald, DH., editor. Developmental and Reproductive Toxicology: A Practical Approach. 2nd. CRC Press; Boca Raton: 2006. p. 467

Porter DW, Hubbs AF, Chen BT, McKinney W, Mercer RR, Wolfarth MG, et al. Acute pulmonary dose-response to inhaled multi-walled arbon nanotubes. Nanotoxicology. 2012; 7:1179–94. [PubMed: 22881873]

Prisby RD, Muller-Delp J, Delp MD, Nurkiewicz TR. Age, gender, and hormonal status modulate the vascular toxicity of the diesel exhaust extract phenanthraquinone. J Toxicol Environ Health A. 2008; 71:464–70. [PubMed: 18306094]

Roberts JR, McKinney W, Kan H, Krajnak K, Frazer DG, Thomas TA, et al. Pulmonary and cardiovascular responses of rats to inhalation of silver nanoparticles. J Toxicol Environ Health A. 2013; 76:651–68. [PubMed: 23941635]

Rogers LK, Velten M. Maternal inflammation, growth retardation, and preterm birth: insights into adult cardiovascular disease. Life Sci. 2011; 89:417–21. [PubMed: 21821056]

Ruehlmann DO, Steinert JR, Valverde MA, Jacob R, Mann GE. Environmental estrogenic pollutants induce acute vascular relaxation by inhibiting L-type Ca2+ channels in smooth muscle cells. FASEB J. 1998; 12:613–19. [PubMed: 9576488]

Sager TM, Castranova V. Surface area of particle administered versus mass in determining the pulmonary toxicity of ultrafine and fine carbon black: comparison to ultrafine titanium dioxide. Part Fibre Toxicol. 2009; 6:15. [PubMed: 19413904]

Sager TM, Kommineni C, Castranova V. Pulmonary response to intratracheal instillation of ultrafine versus fine titanium dioxide: role of particle surface area. Part Fibre Toxicol. 2008; 5:17. [PubMed: 19046442]

Schwartz SM. Role of endothelial integrity in atherosclerosis. Artery. 1980; 8:305–14. [PubMed: 7011261]

Simmons RA. Developmental origins of diabetes: the role of oxidative stress. Best Pract Res Clin Endocrinol Metab. 2012; 26:701–8. [PubMed: 22980051]

Stapleton PA, James ME, Goodwill AG, Frisbee JC. Obesity and vascular dysfunction. Pathophysiology. 2008; 15:79–89. [PubMed: 18571908]

Stapleton PA, Minarchick VC, Cumpston AM, McKinney W, Chen BT, Sager TM, et al. Impairment of coronary arteriolar endothelium-dependent dilation after multi-walled carbon nanotube inhalation: a time-course study. Int J Mol Sci. 2012a; 13:13781–803. [PubMed: 23203034]

Stapleton PA, Minarchick VC, McCawley M, Knuckles TL, Nurkiewicz TR. Xenobiotic particle exposure and microvascular endpoints: a call to arms. Microcirculation. 2012b; 19:126–42. [PubMed: 21951337]

Stapleton PA, Minarchick VC, Yi J, Engels K, McBride CR, Nurkiewicz TR. Maternal engineered nanomaterial exposure and fetal microvascular function: does the Barker hypothesis apply? Am J Obstet Gynecol. 2013; 209:227. e1–11. [PubMed: 23643573]

Thompson LC, Urankar RN, Holland NA, Vidanapathirana AK, Pitzer JE, Han L, et al. C(6)(0) exposure augments cardiac ischemia/reperfusion injury and coronary artery contraction in Sprague Dawley rats. Toxicol Sci. 2014; 138:365–78. [PubMed: 24431213]

Tuma, RF.; Duran, WN.; Ley, K. Handbook of Physiology: Microcirculation. Academic Press; San Diego, CA: 2008.

van den Hooven EH, Pierik FH, de KY, Willemsen SP, Hofman A, van Ratingen SW, et al. Air pollution exposure during pregnancy, ultrasound measures of fetal growth, and adverse birth outcomes: a prospective cohort study. Environ Health Perspect. 2012; 120:150–156. [PubMed: 22222601]

Vedernikov Y, Saade GR, Garfield RE. Vascular reactivity in preeclampsia. Semin Perinatol. 1999; 23:34–44. [PubMed: 10102169]

Vidanapathirana AK, Thompson LC, Odom J, Holland NA, Sumner SJ, Fennell TR, et al. Vascular tissue contractility changes following late gestational exposure to multi-walled carbon nanotubes or their dispersing vehicle in Sprague Dawley rats. J Nanomed Nanotechnol. 2014; 5:201.

Votyakova TV, Reynolds IJ. DeltaPsi(m)-dependent and -independent production of reactive oxygen species by rat brain mitochondria. J Neurochem. 2001; 79:266–77. [PubMed: 11677254]

Wallace DC. Mitochondria, bioenergetics, and the epigenome in eukaryotic and human evolution. Cold Spring Harb Symp Quant Biol. 2009; 74:383–93. [PubMed: 19955254]

Warheit DB, Sayes CM, Reed KL. Nanoscale and fine zinc oxide particles: can in vitro assays accurately forecast lung hazards following inhalation exposures? Environ Sci Technol. 2009; 43:7939–45. [PubMed: 19921917]

Wu G, Bazer FW, Cudd TA, Meininger CJ, Spencer TE. Maternal nutrition and fetal development. J Nutr. 2004; 134:2169–72. [PubMed: 15333699]

Yamashita K, Yoshioka Y, Higashisaka K, Mimura K, Morishita Y, Nozaki M, et al. Silica and titanium dioxide nanoparticles cause pregnancy complications in mice. Nat Nanotechnol. 2011; 6:321–8. [PubMed: 21460826]

Yi J, Chen BT, Schwegler-Berry D, Frazer D, Castranova V, McBride C, et al. Whole-body nanoparticle aerosol inhalation exposures. J Vis Exp. 2013:e50263. [PubMed: 23685643]

Yoshida S, Hiyoshi K, Oshio S, Takano H, Takeda K, Ichinose T. Effects of fetal exposure to carbon nanoparticles on reproductive function in male offspring. Fertil Steril. 2010; 93:1695–9. [PubMed: 19446808]

Zhou M, Diwu Z, Panchuk-Voloshina N, Haugland RP. A stable nonfluorescent derivative of resorufin for the fluorometric determination of trace hydrogen peroxide: applications in detecting the activity of phagocyte NADPH oxidase and other oxidases. Anal Biochem. 1997; 253:162–8. [PubMed: 9367498]

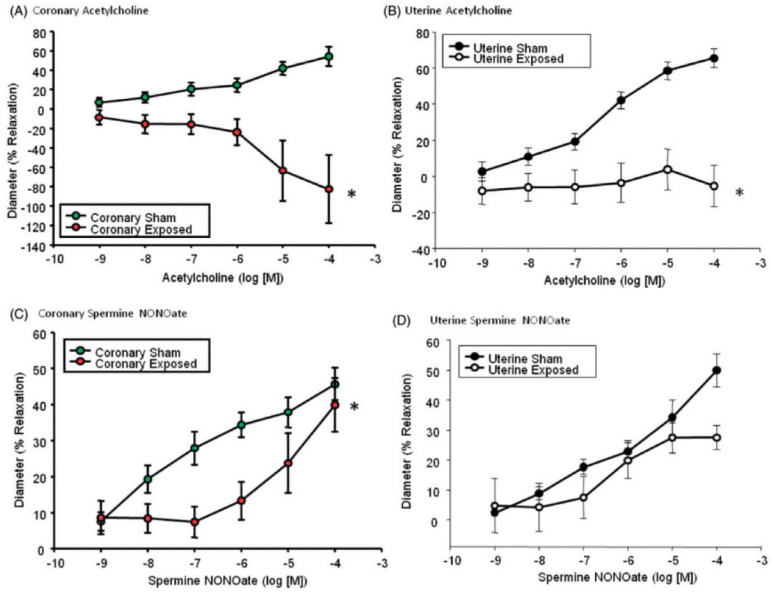

Figure 1.

Chemical agonists of arteriolar dilation. Endothelium-dependent dilation *via* an acetylcholine dose response curve for (A) coronary (N = 7 (sham) and 12 (gestationally exposed) rats; n = 11(sham) and 16 (gestationally exposed) vessels) and (B) uterine (N = 7 (sham) and 12 (gestationally exposed) rats; n = 12 (sham) and 19 (gestationally exposed) vessels) arterioles. Endothelium-independent dilation *via* a spermine-NONOate dose response curve for (C) coronary (N = 7 (sham) and 13 (exposed *in utero*) rats; n = 11 (sham) and 15 (exposed *in utero*) vessels) and (D) uterine (N = 6 (sham) and 11 (exposed *in utero*) rats; n = 11 (sham) and 19 (exposed *in utero*) vessels) arterioles. Values are means ± SE. *$p \leq 0.05$ sham regression line vs. exposed regression line.

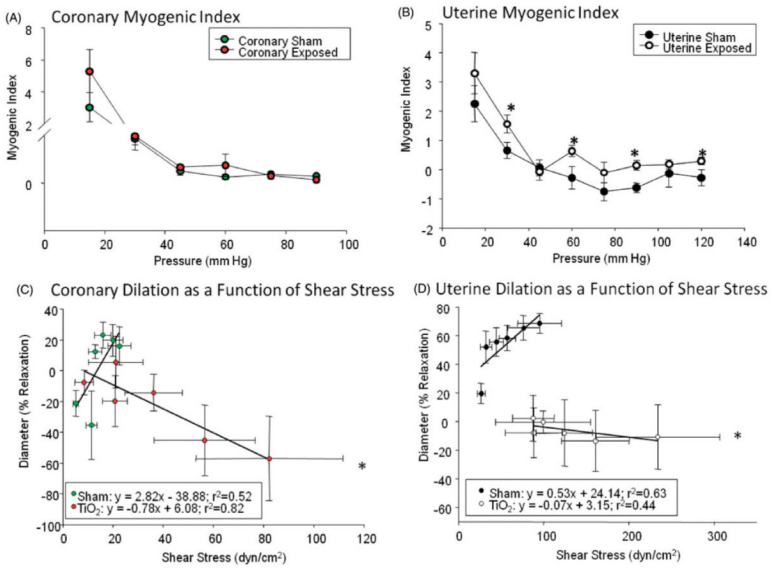

Figure 2.

Mechanical initiators arteriolar responsiveness. Myogenic index calculations for (A) coronary (N = 8 (sham) and 13 (prenatally exposed) rats; n = 11 (sham) and 15 (prenatally exposed) vessels) and (B) uterine (N = 7 (sham) and 10 (prenatally exposed) rats; n = 8 (sham) and 11 (prenatally exposed) vessels) arterioles. Values are means ± SE. *$p \leq 0.05$ two-way ANOVA; arteriolar dilation as a function of shear stress of the (C) coronary (N = 7 (sham) and 8 (exposed *in utero*) rats; n = 11 (sham) and 15 (exposed *in utero*) vessels) and (D) uterine (N = 7 (sham) and 11 (exposed *in utero*) rats; n = 11 (sham) and 11 (exposed *in utero*) vessels) arterioles. *$p \leq 0.05$ sham regression line vs. gestational exposure regression line for both the coronary and uterine arterioles.

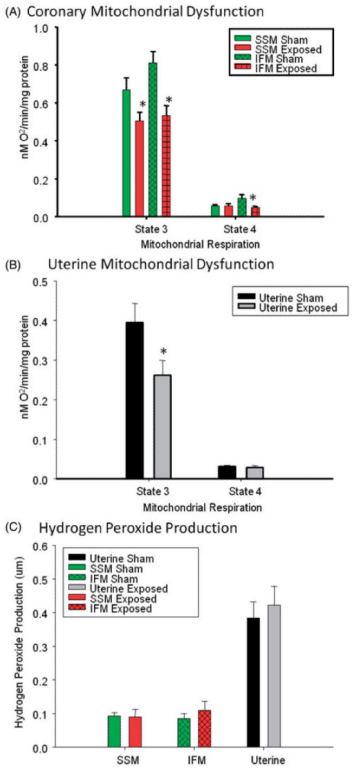

Figure 3.

Mitochondrial dysfunction and reactive oxygen species production. (A) Cardiac subsarcolemmal (SSM) and intramyofibril (IFM) mitochondrial populations and (B) uterine mitochondrial dysfunction of state 3 and/or state 4 respiration. (C) Hydrogen peroxide production within the SSM, IFM and uterine tissues of female progeny after gestational ENM exposure (N = 11–16 rats from 8 to 10 differing litters per group). *Data were analyzed using Student's t-test with $p \leq 0.05$.

Table 1

Maternal, litter and progeny characteristics.

Gestational group	*N* (litters or dams)	Maternal weight (gestational day 20)	Implantation sites	Pups per litter	Progeny weight (week 4)	Progeny weight (week 8)	Progeny weight (week 12)	Progeny weight (week 16)	Progeny weight (week 20)	Progeny avg. age (weeks)	Progeny MAP
Sham	7	429±6.5	12.5±0.42	10.6±0.81	88.76±1.93	219.42±5.41	274.05±7.15	309.27±13.43	319.17±9.02	14.23±1.51	102.89±6.57
Exposed	6	416±16.2	13.3±0.95	10.7±1.08	85.63±1.90	214.71±2.74	254.06±9.51	292.14±9.25	313.50±9.67	13.52±1.2	98.45±2.62

There were no significant differences between sham and exposed litters with respect to litter number, litter loss, growth or age of the female progeny.

Table 2

Vascular characteristics (all).

Vascular bed	Gestational treatment	*N* (adult progeny) 11	*n* (isolated arterioles) 18	Active diameter (pm)	Passive diameter (μm)	Active vessel tone (%)
Coronary	Sham	11	18	113.8±4.6	138.8±4.3	33.3±5.9
	Exposed	15	24	108.9 ±4.9	135.9 ±3.4	28.3 ±2.6
Uterine	Sham	9	16	46 ±5.0	89.6 ±4.2	54.2 ±4.0
	Exposed	14	21	57.1±4.6[a]	85.1±5.9	35.2±2.7[a]

"*N*" represents the number of rats studied and "*n*" represents the total number of coronary-uterine arterioles evaluated per group. One to three arterioles were studied per animal. Values are means±SE.

[a] $p \leq 0.05$ sham vs. exposed.